

Article

Towards Resilient Critical Infrastructures: Understanding the Impact of Coastal Flooding on the Fuel Transportation Network in the San Francisco Bay

Yiyi He ^{1,*}, Sarah Lindbergh ¹ , Yang Ju ² , Marta Gonzalez ³ and John Radke ^{1,3}

- ¹ Department of Landscape Architecture and Environmental Planning, University of California at Berkeley, Berkeley, CA 94720, USA; sarah_lindbergh@berkeley.edu (S.L.); ratt@berkeley.edu (J.R.)
² Institute of Urban and Regional Development, University of California at Berkeley, Berkeley, CA 94720, USA; yangju90@berkeley.edu
³ Department of City and Regional Planning, University of California at Berkeley, Berkeley, CA 94720, USA; martag@berkeley.edu
* Correspondence: yiyi_he@berkeley.edu; Tel.: +1-510-604-7393

Abstract: Sea level rise (SLR) and storm surge inundation are major concerns along the coast of the San Francisco Bay (the Bay Area), impacting both coastal communities and critical infrastructure networks. The oil industry comprises a complex and critical infrastructure network located in the Bay Area. There is an urgent need to assess consequences and identify risk-based solutions to increase the resilience of this industrial network in the Bay Area to SLR and storm surge. In this study, a comprehensive multi-modal network model representing the fuel supply system was built. A total of 120 coastal flooding scenarios, including four General Circulation Models, two Representative Concentration Pathways, three percentiles of future SLR estimates, and five planning horizons (20 year intervals from 2000 to 2100) were considered. The impact of coastal flooding on fuel transportation networks was studied at two different scales: regional and local. At the regional scale, basic network properties and network efficiency were analyzed across multiple flooding scenarios. At the local scale, cascading effects of individual node disruptions were simulated. Based on this research, smarter and more holistic risk-based adaptation strategies can be established which could lead to a more resilient fuel transportation network system.

Keywords: sea level rise; coastal flooding; network modeling; fuel transportation network



Citation: He, Y.; Lindbergh, S.; Ju, Y.; Gonzalez, M.; Radke, J. Towards Resilient Critical Infrastructures: Understanding the Impact of Coastal Flooding on the Fuel Transportation Network in the San Francisco Bay. *ISPRS Int. J. Geo-Inf.* **2021**, *10*, 573. <https://doi.org/10.3390/ijgi10090573>

Academic Editor: Wolfgang Kainz

Received: 1 July 2021
Accepted: 10 August 2021
Published: 24 August 2021

Publisher's Note: MDPI stays neutral with regard to jurisdictional claims in published maps and institutional affiliations.



Copyright: © 2021 by the authors. Licensee MDPI, Basel, Switzerland. This article is an open access article distributed under the terms and conditions of the Creative Commons Attribution (CC BY) license (<https://creativecommons.org/licenses/by/4.0/>).

1. Introduction

Critical infrastructure (CI) is part of the central nervous system of the economy in many developed and developing countries. Although there are many definitions of CI, the first official definition of CI in the United States comes from Executive Order 13,010, signed in 1996, where CI is defined as “the framework of interdependent networks and systems comprising identifiable industries, institutions (including people and procedures), and distribution capabilities that provide a reliable flow of products and services essential to the defense and economic security of the United States, the smooth functioning of government at all levels, and society as a whole.” [1]. Telecommunications, electrical power grids, oil and gas transportation systems, banking and finance institutions, water supply systems, and emergency service networks are all considered to be CIs. It is impossible to achieve the goals of energy stability, and economic or social development, if the operation of the interconnected CI networks is at risk, unstable, or vulnerable [2].

The oil industry is a good example of a sector with complex CI networks, in which any disruption or failure to the process of hydrocarbon discovery, fuel extraction, processing, and distribution can have a significant impact on the industry’s ability to function as a system [3]. Traditionally, this industry sector is subdivided into three segments: upstream, midstream, and downstream [4,5]. The upstream segment manages the exploration and

production of crude oil, the midstream segment refines the crude oil into fuel-based products, and the downstream segment transports the products to end users, such as airports and gas stations. From upstream to downstream, multiple modes of transportation networks are necessary to ensure stable and secure fuel flow from supply to demand. Components of the fuel sector interconnect with one another, forming a complex fuel supply infrastructure network (Figure 1). To increase efficiency, the physical connections and operational interrelations between fuel infrastructure assets tend to be strengthened, promoting the growth of large-scale interconnected systems [6]. However, this connectivity results in an increase in potential uncontrollable risks within the complex CI systems, because the functionality of an individual asset now depends on an ever-increasing number of external assets [7,8].

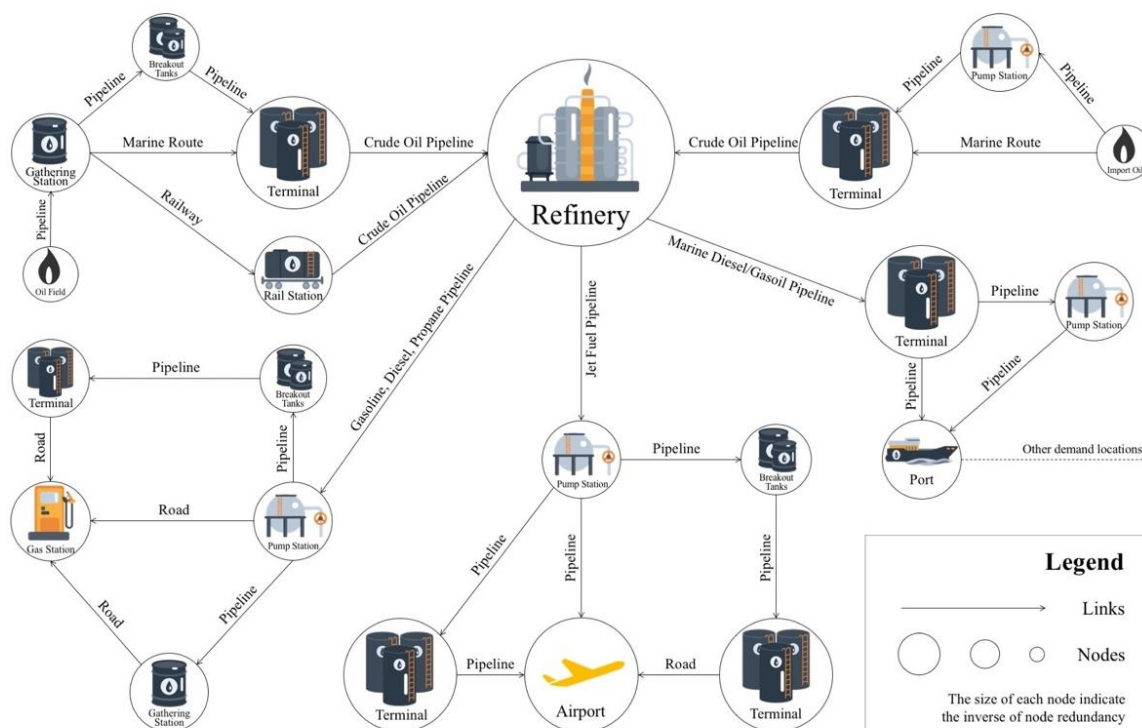


Figure 1. Conceptual visualization of the complex fuel transportation network in the Bay Area. The fuel transportation network is a complex system that consists of various infrastructure assets that can be conceptualized into two categories: nodes and links. Nodes are an abstraction of infrastructure assets where fuel feedstock and products are processed, transferred, stored, or consumed, such as refineries, terminals, ports, airports, and gas stations. Links are an abstraction of key transportation modes, such as pipelines, railways, marine routes, and roads. Fuel feedstock and products travel along these transportation infrastructures from the upstream towards the downstream along the fuel supply chain. Please refer to Appendix A for more details on node and link asset types.

In recent decades, climate change has had an increasing impact on the frequency, intensity, and length of extreme weather events at both global and regional scales. Such impacts are also projected to increase in the coming decades [9–18]. These events, such as heatwaves, extreme storms, and coastal flooding, have had major impacts on the fuel infrastructure networks, causing damage of up to USD 1 billion per event [19,20]. Among these, coastal flooding poses major threats to the U.S. fuel transportation infrastructure and interconnected systems because much of it is spatially proximal to coastlines [21,22]. Global sea level rise is a long-term phenomenon measured from the last glacial maximum, to which ocean's thermal expansion and ice mass loss are major contributors. However, sea level rise differs regionally and locally based on changes in the elevation values of the geoid, changes in sea surface elevation relative to the geoid, and vertical land motion (local sediment compaction, land subsidence, tectonics, and the Earth's deformation based

on ice and ocean mass redistribution). Locally, sea level rise is exacerbated in regions with widespread compacting artificial landfills such as the San Francisco Bay Area [23]. Regionally, recent discoveries in ice loss dynamics reveal that the Californian coast is highly exposed to the most vulnerable major ice sheet loss in West Antarctica. For every meter in global sea level rise induced by the loss of West Antarctica ice, the Californian coast will experience an increase of approximately 1.25 m [24]. Furthermore, the short-term elevations of sea levels from storm surges are also expected to intensify the effects of global and regional sea level rise. Compound effects of long-term rising sea levels, perigean high tides, intense coastal storms, and heavy precipitation events from the Pacific Basin climate fluctuations or winter storms, threaten coastal fuel infrastructure networks as a result of inundation, sloshing, beach erosion, and cliff retreat in California [10,25–27]. Extreme storm surge events at high tides are expected to increase [28], raising the risk of inundating and disrupting interconnected critical energy facilities such as power plants, refineries, pipelines, and transmission and distribution networks. For example, rail transportation lines that carry coal to power plants often follow coastlines and riverbeds (In 2020 alone, the U.S. railroads moved three million carloads of coal, with each rail car carrying enough coal to power 19 homes for an entire year. More than two-thirds (67%) of the coal that was delivered to the U.S. electric power sector in 2020 was shipped either completely or in part by rail; the remainder was shipped by river barge, truck, or other methods [29]). More intense rainstorms can lead to flooding that degrades or washes out nearby railroads and roadbeds [16,30].

In addition, fuel transportation networks are connected and interdependent on other physical and economic systems, many with critical components of fuel supply, such as coal, oil, and electricity. Disruptions in one location in a particular transportation infrastructure network could induce a “ripple effect”, causing damage and failure of varying lengths and magnitudes in dependent or interdependent systems. In 2005, the damage to oil and gas production and delivery infrastructure due to Hurricanes Katrina and Rita affected natural gas, oil, and electricity systems in most parts of the United States [31,32]. Market impacts were felt as far away as New York and New England [33], highlighting the significant indirect economic impacts of climate-related events that go well beyond the direct damages to the infrastructure itself. It is, therefore, paramount to understand the underlying complexity of fuel transportation networks and evaluate the potential impact of these extreme events on the fuel transportation sector under future climate change scenarios. The outcome of such efforts should be made available for the public and policymakers to proactively develop more resilient critical infrastructure networks.

In this study, we reexamined the role of science-based environmental planning in creating more resilient CI networks through a case study of the fuel transportation network in the San Francisco Bay Area (hereafter referred to as the Bay Area). We used the outputs of the state’s latest effort to model coastal flooding impacts on the critical infrastructure (California’s 4th Climate Change Assessment) under 120 climate scenarios, moving from simple place-based analysis to a networked approach where we evaluated the impact of multi-scenario coastal flooding on the multi-modal fuel transportation network as a complex connected system. Evaluation and estimation of uncertainties from both climate variation and network effect perspectives were undertaken. The analytical process and findings from this study offer new insights into understanding, characterizing, and modeling complex CI networks, and highlight the importance of science-based proactive environmental planning that considers both network interdependencies and the challenges posed by future climate change.

2. Materials and Methods

2.1. Fuel Transportation Infrastructure in the Bay Area

Located on the west coast of the United States, the Bay Area has a high concentration of fuel transportation network assets, and houses the second largest refinery complex in the state (a total of 18 refineries are operational in California’s fuel supply chain—the

largest concentration of refineries is in the Los Angeles–Long Beach complex, with a total of nine refineries, whereas the Bay Area complex includes five refineries); five of the nine major ports (there are nine major ports transporting fuel in California—five serve the San Francisco Bay Area from the south bay to Stockton, and the other four are located in southern California between Port Hueneme and San Diego [22]); and nearly half of the terminals in the state of California (Figure 1). These infrastructure assets are especially concentrated in low-lying areas near the coastline where the hazard risk of coastal flooding is high. Figure 2 illustrates the location of node and link assets that compose the fuel transportation infrastructure in the study area. The data relating to these assets were collected from the multiple sources shown in Table 1. Node assets include refineries, terminals, ports, airports, and gas stations. Link assets include marine routes, pipelines (transporting crude oil and finished fuel product), railways, and roads. These assets interconnect with one another, forming a complex network that enables the flow of fuel from supply to demand.

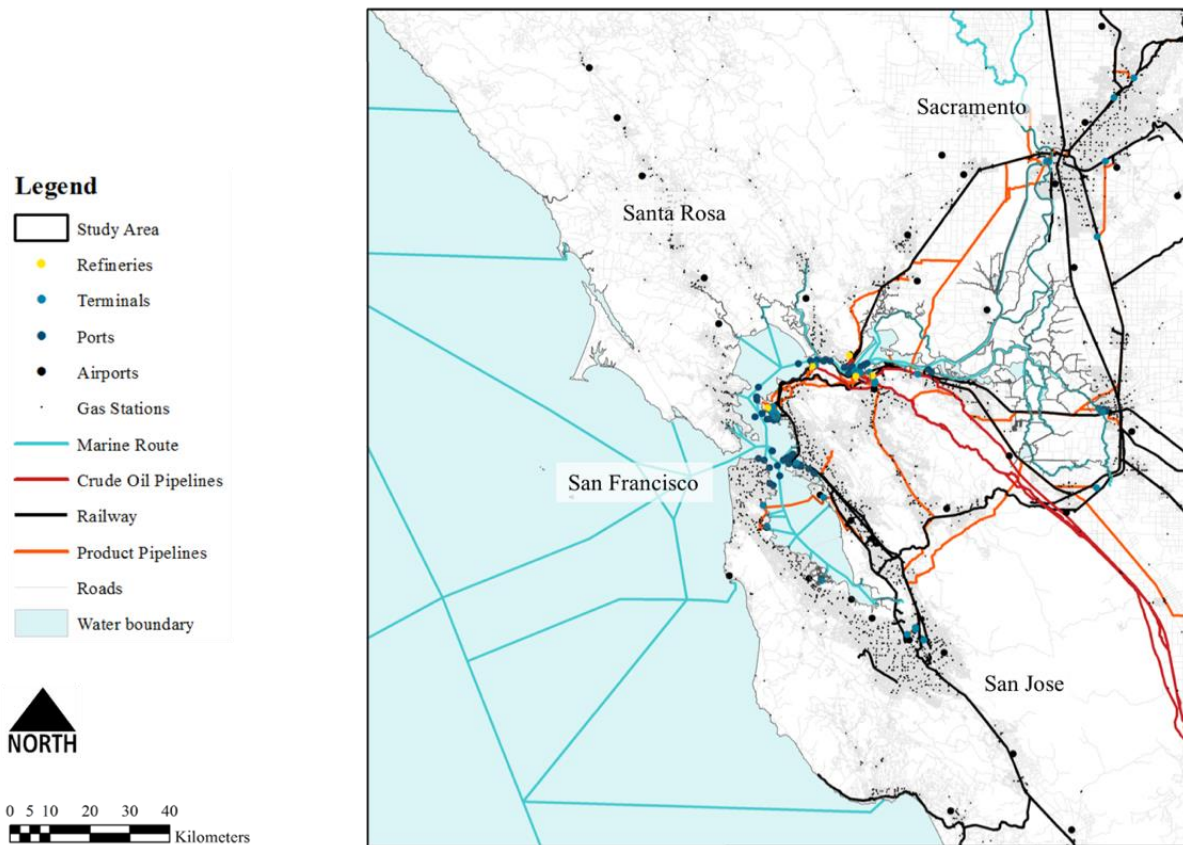


Figure 2. Map of node and link assets that compose the fuel transportation network in the San Francisco Bay study area. The study area is bounded by four geographic coordinate pairs denoted as: [38.902, −123.711], [38.902, −121.051], [36.855, −121.051], and [36.855, −123.711].

Table 1. Data sources for node and link assets collected in the study.

Node Assets		Link Assets	
Refineries	Energy Information Administration	Railways	ArcGIS Business Analyst
Terminals	Energy Information Administration	Pipelines	National Pipeline Mapping System
Gas Stations	Google Places	Roads	Open Street Map
Docks	U.S. Department of Transportation/Bureau of Transportation Statistics' National Transportation Atlas Database	Marine Routes	U.S. Department of Transportation/Bureau of Transportation Statistics' National Transportation Atlas Database
Airports	State of California, Department of Transportation, Division of Aeronautics		

2.2. Coastal Flooding

In addition to identifying and collecting data about the node and link assets that comprise the fuel transportation network, building a comprehensive understanding of future coastal flooding inundation conditions in the Bay Area is also critical in evaluating hazard risk and identifying resilience options for the infrastructure network. To achieve this goal, we leveraged coastal flooding model outputs from a research project led by Radke et al. [22], in which a hydrodynamic model—3Di [34,35]—was used to model coastal flooding for 120 climate scenarios. The 3Di hydrodynamic model was developed by the Delft University of Technology and is a commercial model that dynamically simulates the movement of tides and flood events over digital representations of land surfaces. The inputs of 3Di include time-series water levels to provide boundary forcing to generate water flows, and digital surface data containing topography, bathymetry, and aboveground objects, such as levees, to direct the waterflows. It should be noted that building structures were excluded in our model because they are too granular to be represented. However, critical flood prevention structures, namely levees, are preserved [36]. A unique advantage of the 3Di model for this study is its feasible computation over large regions at fine spatial resolutions, which is enabled by the model's quadtree-based compression algorithm that simplifies the input digital surface while preserving significant topographic variations, such as those from levees [34]. Our model simulates an entire tidal cycle and calculates, in a series of time steps, the flow direction, velocity, and water depth as a flood event progresses. A detailed description of the modeling process is well documented in reference [22] under Appendix A.

In this study, we modeled the depth and extent of coastal flooding induced by climate drivers, including sea level rise (SLR) and intensified storms. We took sea level and climate projections between 2000 and 2100 from California's Fourth Climate Change Assessment [37,38] as inputs and created flood inundation time series maps for:

(1) Two Representative Concentration Pathways (RCPs). An RCP is a greenhouse gas concentration trajectory adopted by the IPCC [10]. Four pathways were used for climate modeling and research for the IPCC fifth Assessment Report (AR5) in 2014. Of these we modeled two: RCP 8.5, portraying a high greenhouse gas concentration scenario with minimal mitigation, and RCP 4.5, representing a mitigation heavy scenario with lower greenhouse gas emission concentrations.

(2) Four General Circulation Models (GCMs). General Circulation Models are mathematical models that represent physical processes in the atmosphere, ocean, cryosphere, and land surface. They are the most advanced tools currently available for simulating the response of the global climate system to increasing greenhouse gas concentrations [10]. The four GCMs we used were HadGEM2-ES, CNRM-CM5, CanESM2, and MIROC5.

(3) Three probabilistic percentile estimates of SLR at 50 m spatial resolution. The three SLR percentiles used in the model were 50%, 95%, and 99.9%. The long term SLR was projected probabilistically for both RCP 4.5 and 8.5 by Cayan et al. based on a method developed by Kopp et al. [38,39], with additional SLR contributions from the loss of Antarctica ice sheets modeled by DeConto and Pollard [40].

The combination of RCPs, SLR percentiles, and GCMs resulted in 24 scenarios of sea level values between 2000 and 2100. This time horizon (2000–2100) was subdivided using 20 year time intervals. For each 20 year interval and each of the 24 scenarios, a high sea level event (i.e., the 72 h period with the highest sea level within the 20 year interval) was selected and the hourly water levels during the event were used as inputs to the 3Di model [22]. In total, there were 120 coastal flooding model outputs (two RCPs \times four GCMs \times three SLR percentiles \times five time horizons), and these were spatially overlaid with the node and link assets of the fuel transportation network to provide robust information on the exposure of infrastructure to coastal flooding under multiple climate scenarios (Figure 3).

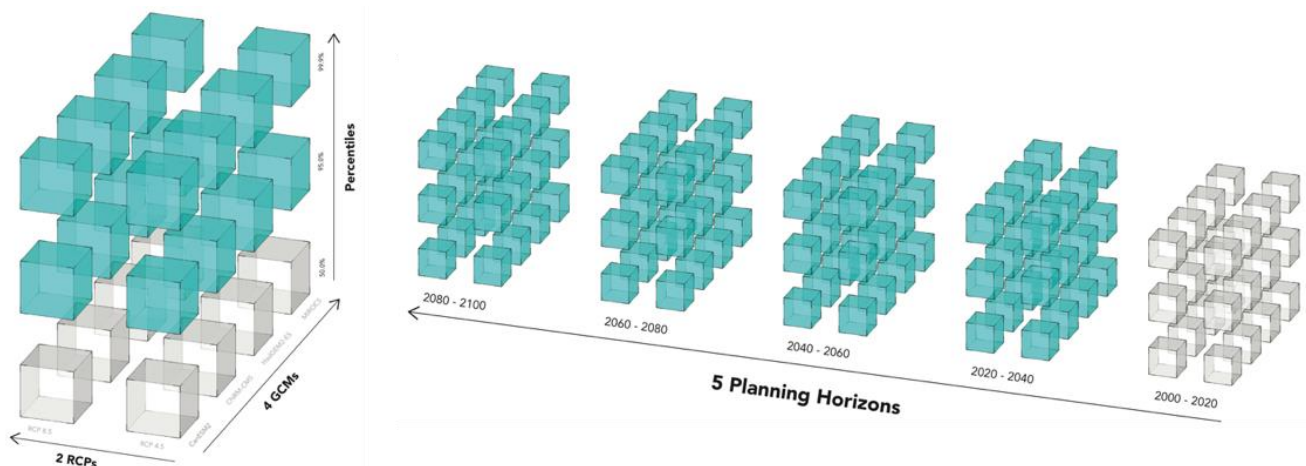


Figure 3. Conceptual diagrams of four GCMs combined with two RCPs, three SLR percentiles projections and five planning horizons. Each cube represents one specific climate scenario. Some cubes are colored blue to illustrate sequential modeling of flooding scenarios. The diagram illustrates the four dimensions of 120 coastal flooding scenarios used in this study.

2.3. Multimodal Network Model

The fuel transportation network is inherently complex with multiple asset types that are interconnected with one another. A major challenge in this study was the creation of a multimodal network that accurately captures the spatial and operational relationships between networked components. We first created a relationship diagram that captures the physical connectivity between asset types following the fuel supply chain from upstream to downstream. Figure 4 shows the relationship between five node asset types and five link asset types of the fuel transportation network in the study area. The lines between node and link assets define physical connections between different asset types. For example, ports such as the Richmond Long Wharf are physically connected to a crude oil pipeline that transports crude oil to the Chevron Richmond refinery. Therefore, we observe connections between (1) port and crude oil pipeline, and (2) crude oil pipeline and refinery. It should be noted that each link asset type represents one layer of the transportation network in the multimodal network model and there is no direct connection between these layers. The node asset types connect different transportation layers, thus forming a network structure similar to a multiplex network. The main difference between the fuel transportation network structure created in this study and the standard multiplex network is the addition of node asset types (port, terminal, refinery, airport, and gas station) as connecting points between different network layers, rather than direct connections between nodes in the subnetwork layers [41–43].

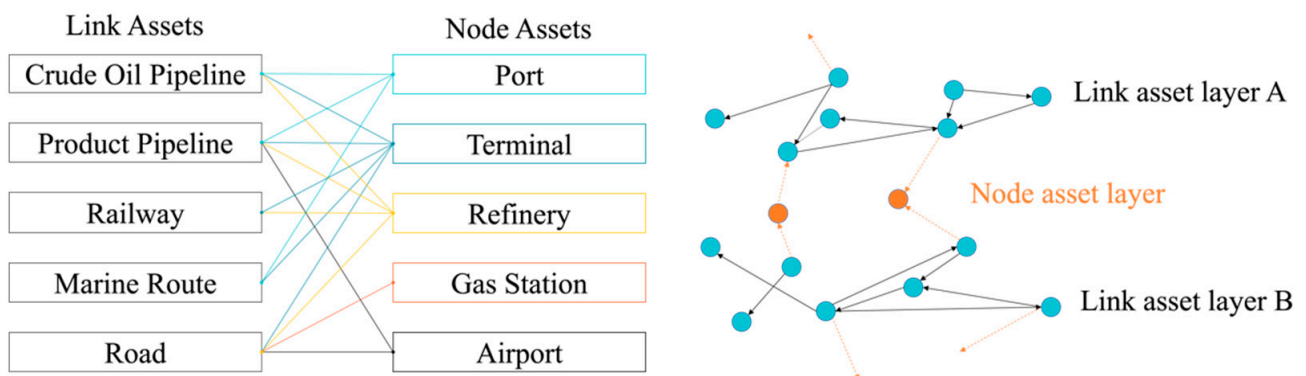


Figure 4. Relationship diagram of the node-link connectivity of the fuel transportation network in the Bay Area (left panel) and simplified example of the connection between node and link assets in the fuel transportation network model (right panel).

After the connection was validated for each pair of node and link assets, we constructed a network model that was able to capture the interconnections within the fuel transportation networks. In this study, a multimodal fuel transportation network was constructed as a directed graph using NetworkX, which is a Python package for the creation, manipulation, and study of the structure, dynamics, and functions of complex networks [44]. In NetworkX, the structure of a network, or graph, is encoded in the links (connections, edges, arcs) between nodes (vertices). It provides basic network data structures for the representation of simple graphs, directed graphs, and graphs with self-loops and parallel edges [44]. The node and link infrastructure assets previously collected were loaded as inputs into NetworkX. The link asset types were first mapped in topographic form and then inserted into the graph as subnetwork layers with nodes and links. The nodes within these subnetworks represent the vertices of line infrastructure segments (e.g., connection points between pipeline segments). The direction of each link follows the fuel supply logic from upstream to downstream. For example, the road network layer consists of intersections represented as nodes and road segments represented as links. Next, the node assets were inserted into the graph connecting different link asset layers following the relational diagram in Figure 4. For example, the refinery connects four different link asset layers/subnetworks, namely, crude oil pipeline, product pipeline, railway, and road. Table A1 shows five types of line assets in their original data format, geographic representation, and topographic representation (graph). Detailed documentation of this process is summarized in Table A2.

The final multimodal fuel transportation network in the study area has 1455 nodes and 1797 links. The average node degree (where the degree of a node equals the number of edges connected to the node) is 2.74 and the average path length (the average path length is defined as the average number of steps along the shortest paths for all possible pairs of network nodes; this is a measure of the efficiency of information within a network) is 14.75. Most nodes have a relatively low degree (fewer than four), yet a small number of nodes have a degree greater than ten, with 17 the maximum (Figure 5). From a network science perspective, nodes with higher degrees are generally considered “hubs” within the network. Figure 6 shows a topologic visualization of the multimodal network where the hubs within the network are individually identified. It is evident that terminals (BNSF rail terminal, Kinder Morgan Concord terminal, Nustar Energy Crockett terminal, and Buckeye Sacramento terminal), refineries (Valero Benicia refinery and Shell Martinez refinery), and ports (Port of Richmond and Port of Oakland) have more connections than other nodes within the network. This result aligns well with knowledge gained from stakeholder interviews [22]. Terminals and ports are critical assets to the operational success of the fuel transportation network because they connect crude oil supply (upstream to midstream) to refined fuel products’ distribution (midstream to downstream). Refineries are the central nodes in the fuel supply–demand chain because they connect upstream supply to downstream demand. Each drop of crude oil must pass through the refining process before it reaches consumers.

To gain a better understanding of the impact of coastal flooding on the fuel transportation network, we spatially overlaid the 120 flood model outputs onto the multimodal network. For each node and link within the network, flood water depth (under 120 scenarios) was extracted and attached to the node or link as an attribute. Our model assumes assets exposed to one meter or more of inundation depth are likely to suffer disruption or failure. This assumption does not take into consideration the diverse impact typologies of coastal flooding on different fuel assets. For example, for assets that are entirely underground, such as pipeline segments, inundation depth is not as relevant a damage typology as erosion and sloshing hazards. Alternatively, for road assets where fuel trucks operate, the minimum flood impact threshold may be lower [45]. For marine routes, for example, increase in sea levels does not represent any damage potential per se but could induce changes in vertical clearance restrictions for large fuel tankers circulating the Bay Area. Therefore, all nodes and links shown to have greater than one meter floodwater inundation

were removed from the network. As a result, a total of 120 “impacted” networks were created in which regional and local effects of an assumed disruption given one meter inundation depth could be assessed for each coastal flooding scenario.

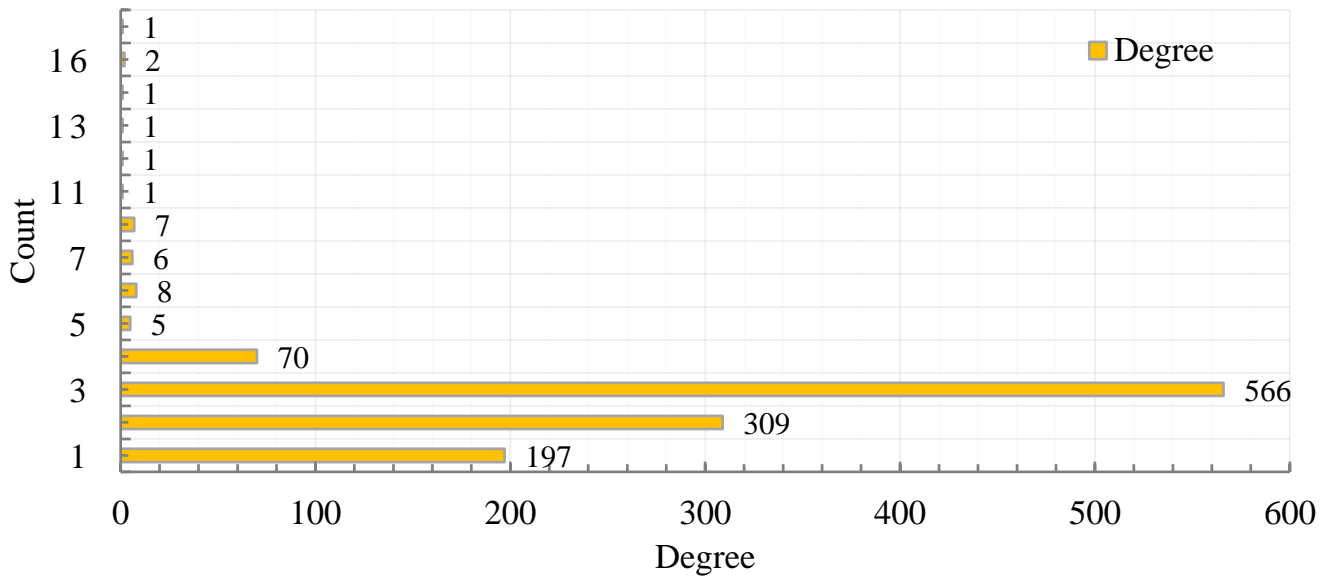


Figure 5. Node degree distribution of the fuel transportation multimodal network.

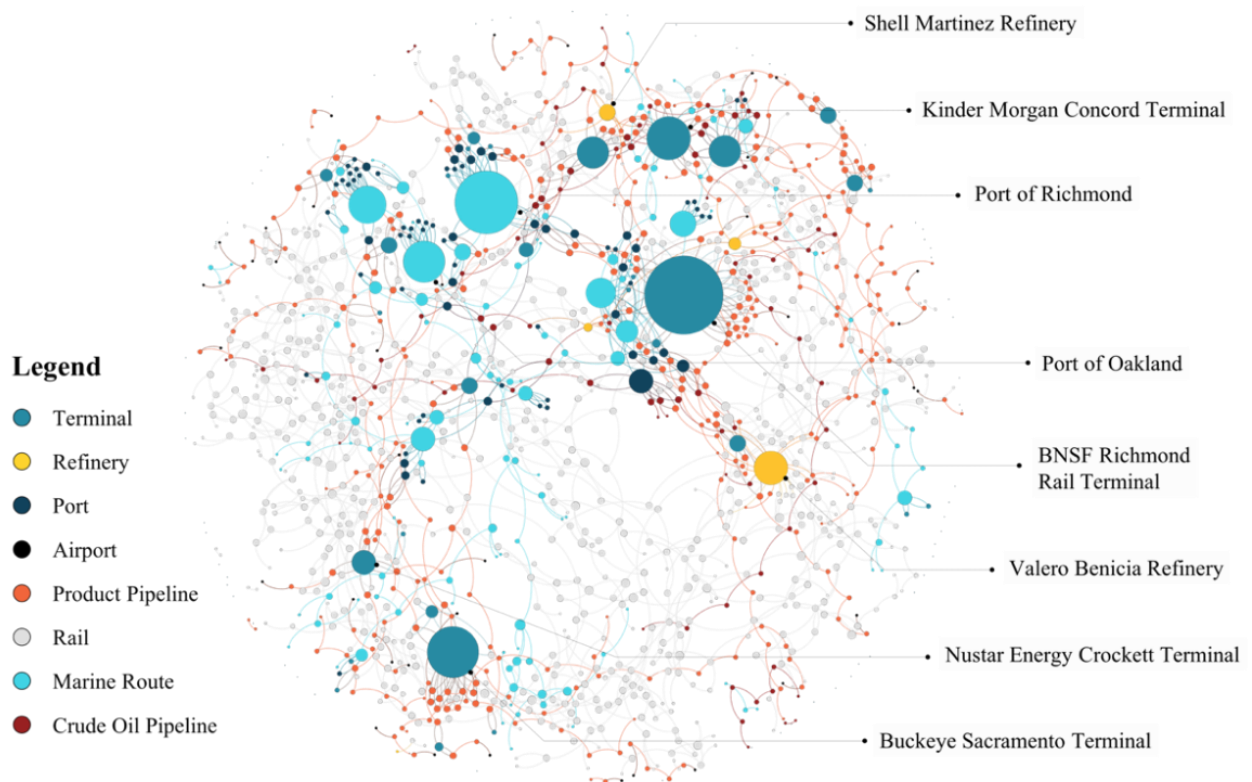


Figure 6. Topologic visualization of the fuel transportation network in the study area. Each circle represents a node within the network. All nodes are color coded according to the type of asset they represent. The size of the circle corresponds to the degree of each node: bigger circles represent nodes with a higher degree (more connections) whereas smaller circles represent nodes with a lower degree (fewer connections).

2.4. Flood Impact Analysis

We studied flood impact at two scales: regional and local. The regional scale analysis focuses on measuring the impact of coastal flooding in terms of hazard exposure and changes in network level properties over time (from 2000 to 2100) and under different GCMs and RCPs scenarios. This process is broken down into three sections: (1) measuring the change in the total number of nodes and links; (2) measuring the change in the number of connected components; and (3) measuring the change in network efficiency. The first section aimed to evaluate the total place-based exposure of the nodes and links within the network under 120 flooding scenarios. This was achieved by subtracting the remaining number of nodes and links from the original count that is not impacted by coastal flooding. The second section aimed to explore whether the network becomes more fragmented under various coastal flooding scenarios. Initially, the network is fully connected as one component. However, if nodes within the network are disrupted by coastal flooding, and therefore removed from the network, the network may break down into several components or sub-networks. As a result, the routes between nodes will be impacted and the performance of the network will decrease due to connectivity-based impacts. To test whether coastal flooding impact on the fuel transportation multimodal network will cause network fragmentation, the number of connected components was calculated. The third section aimed to measure how the efficiency of the network changes over time. In this study, Global Efficiency (GE) was used to quantify the changes in the efficiency of the network under different flooding scenarios. The GE of a network, first proposed by Latora and Marchiori [46], is a measure of the exchange of information within a network. Osei-Asamoah et al. [47] explained that GE quantifies how flow is exchanged between nodes in a transportation network. Specifically, the GE of the network is defined as:

$$GE = \frac{1}{N(N-1)} \sum_{s \neq t} \frac{1}{Z_{st}}$$

where: Z_{st} is the length of the shortest path between node s and node t ; N is the number of nodes in the network.

The GE value obtained was normalized (min = 0, max = 1) by dividing by the GE of an ideal network in which all node pairs are connected. Using the equation introduced above, the global efficiency of all 120 impacted networks was calculated.

The local impact analysis focuses on the ripple effects due to disruptions of a particular node within the network. This process was modeled based on the connectivity within the original multimodal network. If one node is disrupted, then this node was identified as the 1st “ripple”, and all nodes that were directly connected to this node were labeled as the 2nd ripple. Similarly, the nodes that were connected to those identified as the 2nd ripple were labeled as the 3rd ripple. This process was repeated until there were no other nodes left that were connected to all previous nodes. In reality, fuel constantly flows through the multimodal network from supply nodes to demand nodes with minimal stopping points. The above-described model can approximate the downstream impacts of local network failures.

3. Results

3.1. Regional Impact

At the regional level, the impact of coastal flooding on the multimodal network was first measured by evaluating the number of nodes and links that are directly exposed. Figure 7 shows the result of node and link exposure across five time horizons. Overall, we observe an uprising exposure pattern across both node and link assets over time. The RCP 8.5 scenarios have relatively larger exposure profiles than RCP 4.5 scenarios. Given the same RCP, the 95th and 99.9th percentile sea level rise scenarios have a relatively larger impact than the 50th percentile scenario. Furthermore, the variation in hazard exposure for both node and link assets to coastal flooding also increases over time and is smaller for the first two time horizons and larger for the following three time horizons.

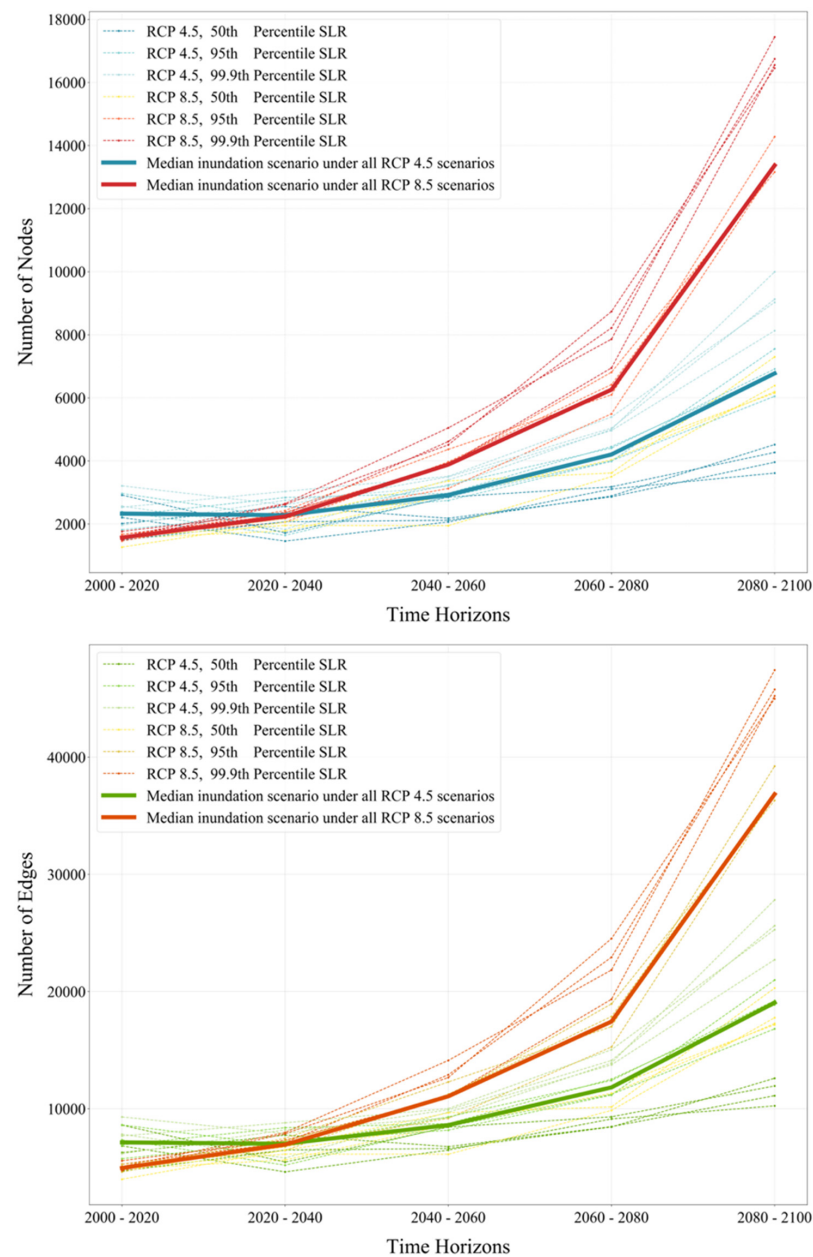


Figure 7. Node (top panel) and link (bottom panel) infrastructure asset exposure to 120 coastal flooding scenarios. The horizontal axis shows the five time horizons and the vertical axis shows the count of node and link assets. Median inundation scenarios under RCP 4.5 and RCP 8.5 are also included.

The percentage of nodes and links that are impacted by different coastal flooding scenarios were also calculated and categorized according to the type of asset they represent (Figure 8). On average, link assets have greater exposure to coastal flooding compared with node assets. Among all asset types, product pipelines have a higher percentage of hazard exposure, whereas refineries have a relatively lower percentage exposure. When compared across different time horizons, all asset types experience a higher percentage of flood hazard exposure towards later time horizons. The variation of exposure (within the same time horizon) increases over time due to the uncertainties in future climate projections. A similar pattern can also be observed for the count of the number of connected components, in which the potential variation resulting in a fragmented network after disturbance by coastal flooding dramatically increases in later time horizons (Figure 9). In particular, in the first time horizon (2000–2020), the network generally remains as one fully connected

network. However, in later time horizons, the total number of connected components within the multimodal network and its variation within the given time horizon starts to increase. This result suggests that, due to coastal flooding, the multimodal network becomes increasingly fragmented over time with increasing variation. Such a result is to be expected because short-, mid-, and long-term impacts of climate-change-induced extreme weather events, namely, coastal flooding, were not fully accounted for when the fuel transportation network was first designed.

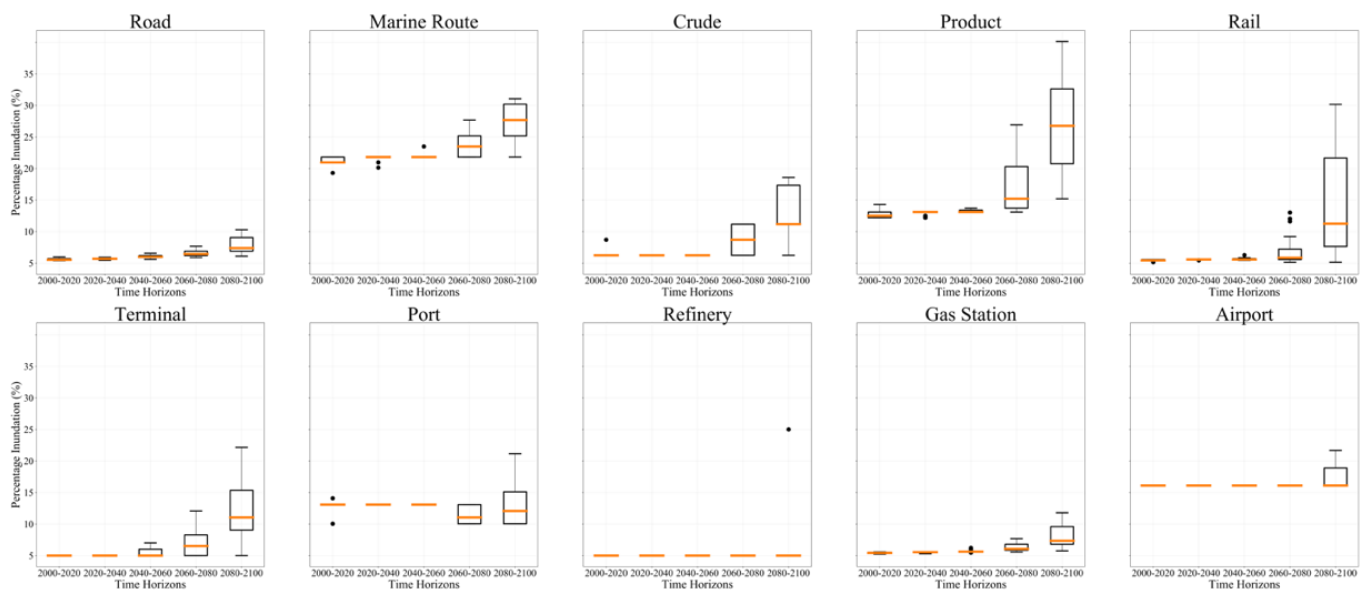


Figure 8. Exposure of node and link fuel infrastructure assets to coastal flooding under 120 climate scenarios. The top row displays boxplots of link asset types’ exposure profiles in terms of percentage inundation and the bottom row displays boxplots for node asset types.

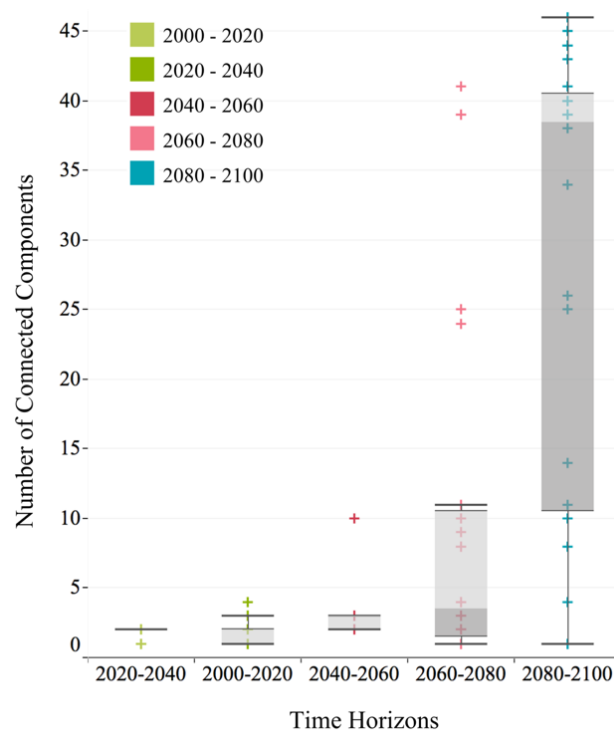


Figure 9. Changes and variations in the number of connected network components over five time horizons.

The global efficiency metric measures and compares flow exchanges between nodes across different time horizons (Figure 10). Our results show that, in general, the efficiency within the multimodal network decreases over time for both RCP 4.5 and RCP 8.5 scenarios. For the first three time horizons (2000–2020, 2020–2040, and 2040–2060), network efficiency remains stable. For RCP 4.5 scenarios, a steep drop in network efficiency occurs during the last time horizon (2080–2100); however, for RCP 8.5 scenarios, the drop in network efficiency happens earlier in the fourth time horizon (2060–2080). In the last time horizon, the minimum value for global efficiency is higher compared with the fourth time horizon. This is potentially caused by the significant divergence between RCP 4.5 and RCP 8.5 after the third time horizon (Figure 7), which results in heterogeneous exposure of fuel transportation infrastructure to coastal flooding under different climate scenarios. As previously mentioned in Section 2.4, the shortest path distance between node pairs is a key component of the global efficiency metric. It is possible that the shortest path distances for some node pairs are reduced in some flood scenarios, resulting in a higher global efficiency value.

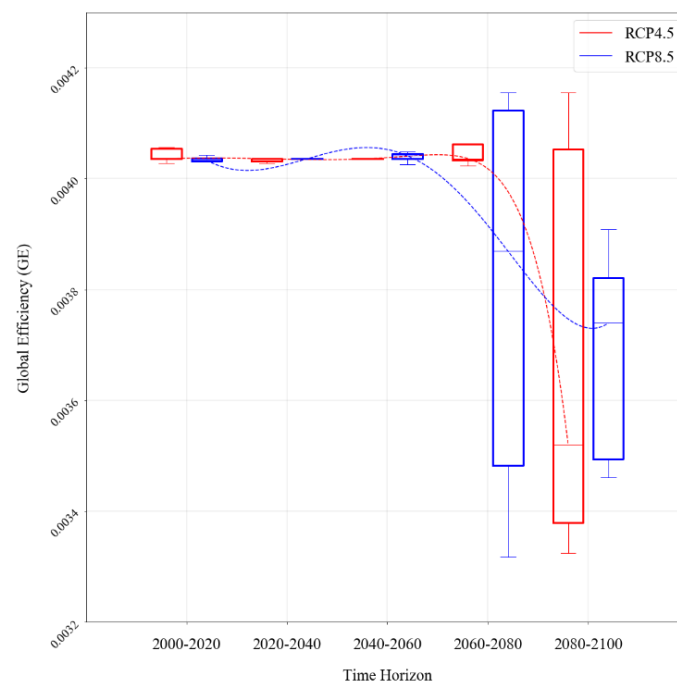


Figure 10. Changes in network global efficiency over five time horizons grouped by RCP 4.5 and RCP 8.5 scenarios. A second-order polynomial is used to achieve a linear fit line demonstrating the overall trend in global efficiency.

3.2. Local Impact

At the local scale, the “ripple” effect caused by node asset failures on individual node and link assets within the fuel transportation network was calculated and visualized (Figure 11). Our results show that the potential impact of local coastal flooding disruptions is greater than that observed in previous hazard exposure analysis. Although a particular node in the multimodal network is not directly exposed to coastal flooding, it might still experience disruptions due to network connectivity. In addition, it is commonly assumed that nodes with a higher degree (‘hubs’ within the network) will likely cause a larger ripple effect in terms of the total number of nodes that are indirectly impacted. However, the results show that this might not always be the case. Some nodes within the network might have a relatively low degree; however, the number of nodes that are impacted indirectly due to a disruption to this node may be large. For example, the Valero Benicia refinery has a relatively low degree compared with the BNSF rail terminal, yet the total number of nodes that would be impacted due to local failure in the refinery is larger than that of the rail terminal.

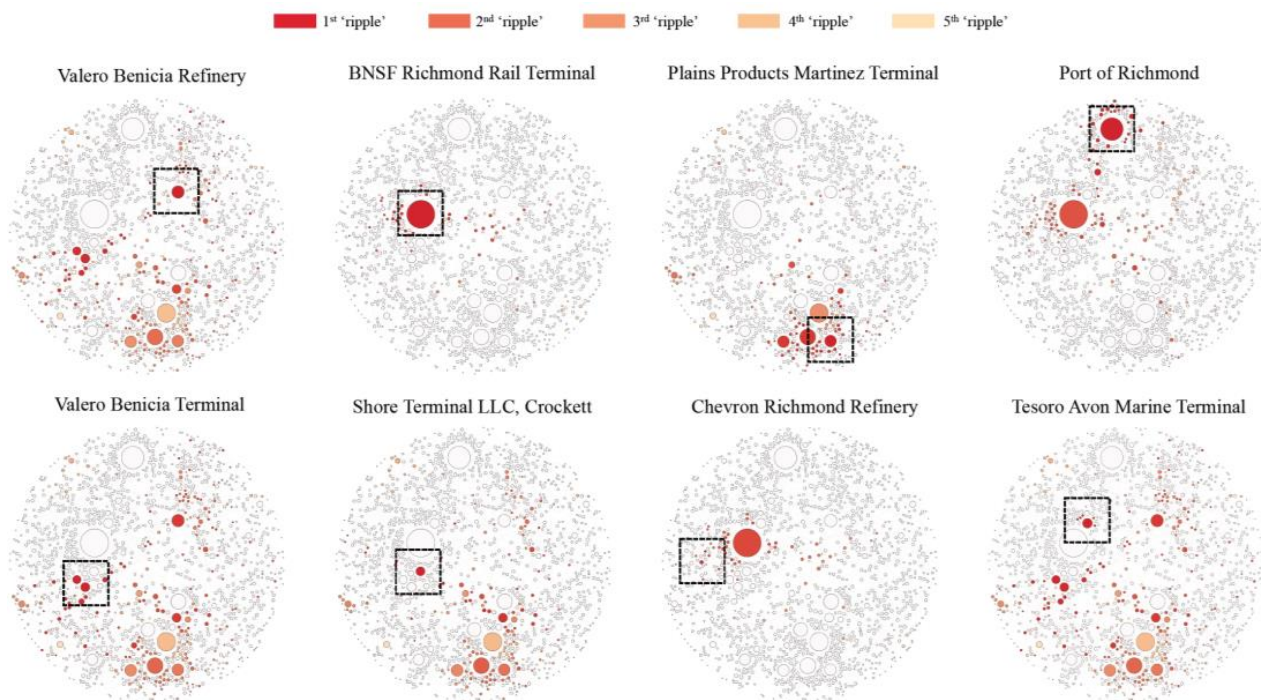


Figure 11. Examples of “ripple” effects within the multimodal network due to simulated local node failures. The nodes are represented using circles and the size of circles corresponds to the degree of the node. The node in the center of the black box is the one that is disrupted by coastal flooding.

4. Discussion

To the best of our knowledge, this study is one of the first attempts to understand what the fuel transportation multimodal network is and how coastal flooding under future climate scenarios impacts the CI network regionally, considering its interdependencies between upstream and downstream infrastructures in the Bay Area. There are limitations in our analysis that can be improved with future research. First, this study only considers the impact of coastal flooding on the multimodal network. However, in coastal regions, infrastructure networks are also vulnerable to inland flood hazards during extreme weather events. Future research should model and measure the impact of both coastal and inland flooding on fuel transportation multimodal networks under various climate scenarios. Our preliminary experiments in the Bay Area using the 3Di hydrodynamic model that created the 120 coastal flooding scenarios show impact potential from inland flooding caused by extreme precipitation events. Second, although real-time fuel flow data is disclosed at fuel asset owner and operator organization levels, a deeper understanding of the fuel flow rates (volume transported in time units) is necessary to foster better contingency plans in case of network disruptions to the fuel distribution. Fuel flow is essential to measure capacity, asset criticality, and network robustness, using the steps implemented in private organizations, but at the Bay Area level. Multiple network simulations should be employed so that the region can better cope with fuel shortage events by understanding: (1) how to redirect fuel flow in case of a node and/or link disruption; (2) whether there exist reliable alternative routes or alternative transportation modes for fuel distribution; and (3) which routes are critical in terms of redundancy or alternative routing. Third, this analysis only incorporates flood depth as the coastal flooding hazard element. It assumes a one-meter depth threshold to all fuel asset types to model disruption scenarios. A finer assessment of damage typologies is needed to better understand how flood depths, flood-water dynamics, duration, erosion, and other coastal flooding dynamics can impact the diverse range of infrastructure assets that comprise the transportation fuel sector. Finally, by better understanding coastal flooding damage typologies and integrating fuel flow disruptions at the network level, future emergency planning can be enhanced via

National Infrastructure Protection Plans and Energy Sector-Specific Plans formulated by the Department of Homeland Security, and state-level emergency training, such as California's Emergency Fuels Set-A-Side Exercises [48–50].

5. Conclusions

Based on the analysis above, four main conclusions can be drawn:

First, the expected impact of coastal flooding on the fuel transportation multimodal network increases over time with more uncertainty. The regional analysis results show that the total number of nodes and links directly exposed to coastal flooding increases over time. When examining the percentage of flood exposure by asset type, the same temporal pattern remains. Overall, RCP 8.5 scenarios would have a bigger impact on the network than the RCP 4.5 scenarios. Given the same RCP, a higher percentile of sea level rise estimation would result in a bigger impact on the multimodal network. Among all types of assets, product pipelines are the most exposed to coastal flooding in terms of average inundation percentage.

Second, the multimodal network is likely to become more fragmented in the future and network efficiency is likely to decrease over time, particularly during the last two time horizons (2060–2080 and 2080–2100). Based on the results of this study, the number of connected components within the multimodal network increases, suggesting that the network is breaking apart, and forming many smaller sub-networks that are not connected to one another. This also suggests that the number of all possible paths within the network will decrease, leading to a drop in global efficiency. A steep drop in network efficiency during the last two time horizons suggests that the exchange of flows within the network will be hindered due to coastal flooding.

Third, when taking the ripple effects within the network into consideration, the real impact of coastal flooding is much larger. One of the key characteristics of the fuel transportation multimodal network is that all node and link assets are fully connected with one another. Nodes within the network depend on many other nodes and links to maintain normal operations. If a disruption occurs to one of the nodes, it is possible that other nodes that are connected to this disrupted node will also be negatively affected. In other words, even though a node in the network is not directly exposed and affected by coastal flooding, it may still be impacted due to connectivity. Additionally, when comparing the ripple effect of a node disruption based on the total number of nodes that will be impacted, the local results show that smaller hubs within the network may cause a larger ripple effect than some of the biggest hubs.

Finally, there are different sources of uncertainty in coastal flooding projections and fuel transportation multimodal network exposure. Regarding network asset exposure to coastal flooding, there is significant variation over the five time horizons. This stems from the uncertainty embedded in global climate models, sea level rise estimates, and carbon emission projections. From the first time horizon (2000–2020) to the final time horizon (2080–2100), the variation in asset exposure to coastal flooding increases dramatically. The uncertainty of the projected coastal flood models of the Bay Area identifies how infrastructure exposed to the median coastal flooding scenario varies between 20 and 54% during the period 2080–2100 under RCP 4.5, and between 40 and 67% for the same period under RCP 8.5 [36]. The long-term variability in the exposure results (from the mid-21st century onward) stems mostly from the choice of RCP scenarios. The same pattern is observed for the percentage of asset exposure, the total number of connected components, and the network global efficiency. The short-term variability in the exposure results (first two time horizons) is derived predominantly from the inherent approximations of the Earth systems' complex interacting processes [24].

In summary, this paper proposes a science-based environmental planning approach to understand the impact of coastal flooding on the fuel transportation network under multiple climate scenarios for the Bay Area. The approach developed in this study goes beyond the traditional place-based approach, in which risk is only assessed for assets directly exposed to hazard areas. A network model is proposed to capture complex interdependencies

of the fuel CI and to model the ripple effects of local network disturbances. This approach and its results play an important role in (1) forming a comprehensive vulnerability and risk profile for infrastructure network components, and the infrastructure network as a whole; (2) measuring uncertainty in the potential impacts of sea level rise combined with climate-change-induced coastal flooding on complex infrastructure; and (3) identifying resilience options and proactive planning strategies towards more resilient fuel supply systems for emergency management and other CI networks.

Author Contributions: Conceptualization, Yiyi He; methodology, Yiyi He, Marta Gonzalez, and John Radke; software, Yiyi He and Yang Ju; validation, Yang Ju; formal analysis, Yiyi He; investigation, Sarah Lindbergh, Yiyi He, Yang Ju, and John Radke; resources, John Radke; data curation, Yiyi He, Sarah Lindbergh, and Yang Ju; writing—original draft preparation, Yiyi He; writing—review and editing, Sarah Lindbergh, John Radke, Yang Ju, and Marta Gonzalez; visualization, Yiyi He; supervision, Marta Gonzalez and John Radke; project administration, John Radke and Marta Gonzalez; funding acquisition, John Radke. All authors have read and agreed to the published version of the manuscript.

Funding: This research was partially funded by the California Energy Commission (PVEA), grant FED-15-001.

Institutional Review Board Statement: Not applicable.

Informed Consent Statement: Not applicable.

Data Availability Statement: Coastal flooding outputs from 3Di can be found here: <http://keystone.gisc.berkeley.edu/>.

Acknowledgments: We would like to thank the Beatrix Farrand Research Fund, University of California at Berkeley, for providing publication funds.

Conflicts of Interest: The authors declare no conflict of interest.

Appendix A

Node assets:

1. Refinery: Refineries are the central node in the fuel supply chain system because they are the convergence points between crude oil feedstock supply and fuel product distribution. It is a complex industrial facility where raw crude oil is converted by a range of different processes into usable fuel products [51]. In California, refineries are mainly concentrated in the San Francisco Bay area, Los Angeles area, and the Central Valley. Two million barrels of petroleum are processed into a variety of fuel products, with gasoline representing about half of the total product volume [52]. In the global oil industry, an oil barrel is defined as 42 US gallons, which is about 159 L or 35 imperial gallons.)
2. Terminal: A terminal facility may have various meanings or functionalities depending on the organization that works with them. They represent a highly complex component of fuel transportation networks because they are functionally distinct, both in terms of the mode involved and the commodities that are being transported [53]. There is no single definition of a terminal. Different agencies and institutions define “terminal” differently according to their specific criteria. In this study, we define terminals as locations in the fuel transportation networks in which liquid bulk fuel commodity originates, terminates, or is handled in the supply and distribution process [22]. They are a type of intermediary facility in the fuel supply system to transport fuel from one node to another. They can be used to transport fuel within the same mode of transportation or between different modes of transportation.
3. Port: In the state of California, ports are usually located along the coast and are fully connected with the marine transportation network, and the crude and product pipeline network. According to the California Department of Transportation (DOT), there are 213 port facilities that handle fuel products within the state. These ports can be used as crude oil unloading terminals, intermediate fuel transloading facilities, or

- destinations for refined fuel products. For example, the Richmond Long Wharf (RLW) near the eastern terminus of the Richmond San Rafael Bridge is one of the largest ports in California, with six berths for receiving crude oil and shipping refined fuel products. It is connected to the Chevron Richmond refinery via a three-foot diameter pipe, moving an average of 10,000,000 gallons of crude oil per day off tanker ships, primarily from Alaska and a small number from the Middle East, to the refinery [54].
4. Gas station: Gas stations or retail fuel outlets are considered to be one type of end consumer node of the fuel supply network in this study. According to the California Retail Fuel Outlet Annual Reporting, there are 10,202 fuel stations that sell gasoline, diesel, and other transportation fuel to the end users within the state [55]. After crude oil is refined at the refinery, fuel products such as gasoline and diesel are transported through product pipelines to terminals. Then, these products are offloaded onto tank trucks through racks at the terminal and then delivered to gas stations. Almost all gas stations within the state receive fuel delivery by tank trucks via the road network.
 5. Airport: Airports in California are huge consumers of fuel: aviation gasoline (AvGas) and jet fuel. According to Caltrans, there are approximately 200 commercial airport facilities within the state that integrate the National Plan of Integrated Airport Systems and thus are classified for functions that require fuel storage facilities within their premises. Other primary jet fuel endpoints in the state are the 23 military airports [56]. In contrast to gas stations, airports usually rely on product pipelines for fuel transport. A majority of jet fuel is transported via a pipeline from the refinery to an intermediated terminal before it is distributed to the airport [22].

Link assets:

1. Pipeline: The U.S. has the world's largest network of energy pipelines. Pipelines are one of the most cost-efficient means of transporting energy fuels and are critical to the oil industry. There are two general types of energy pipelines—liquid petroleum pipelines and natural gas pipelines. In this research, we only studied the former type of pipeline network. The liquid petroleum pipeline network comprises crude oil lines, refined product lines, etc. In California, there are nearly 6000 km of crude oil pipelines in service or idle [57]. Crude oil pipelines are mainly used to transport crude oil from either marine oil terminals or inland terminals to refineries. For example, when Alaskan crude oil arrives at the Richmond Long Wharf, it is transported via a crude oil pipeline directly to the Chevron Richmond refinery. Regarding product pipelines, Kinder Morgan operates over 60% of the product pipeline network in California, followed by Chevron, Shell, and ExxonMobil, which operate between 5–10% each. Phillip66, Andeavor, and the Department of Defense operate between 1–5% each of product pipeline transects [22]. These product pipelines are used to deliver various types of refined fuel products, such as gasoline, diesel, and jet fuel, to the end nodes of the supply chain: gas stations, airports, etc.
2. Road: Among all modes of fuel transportation networks, the road network has the highest density, which translates into higher redundancy and flexibility in case of a link asset disruption. It is well connected to many types of nodes within the fuel transportation network. Different trucking companies operate in different areas of the state to move the finished products from intermediary distribution terminals to the consumer. This mode of fuel transportation does not compete with other modes that are designed for long-haul movements, and is thus limited to shorter distance distributions.
3. Rail: The railway is an important part of fuel transportation networks. A portion of the crude oil supply to California depends on the railway system. There are some crude railway terminals along these railway lines equipped with a rail yard for transloading fuel to other modes of transportation, such as the crude oil pipeline network. The two main rail operators in the state that work with crude oil transportation are Union Pacific Railroad (UP) and Burlington Northern Santa Fe Railways (BNSF).
4. Marine route: The marine transportation network is also one of the most cost-efficient ways of transporting liquid fuels. It is connected to the larger fuel transportation

network system through ports and marine terminals. These routes can be used to bring crude oil from out-of-state supply locations to California and they are also used to transport refined fuel products from refineries to other demand nodes. For example, 80% of the crude oil shipment to southern California arrives at Long Beach Terminal 1/Berth 121 via the marine network.

Table A1. The process of creating topological representations of line asset types.






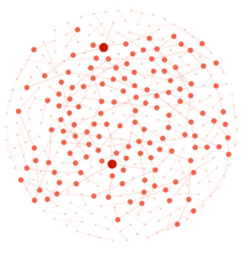


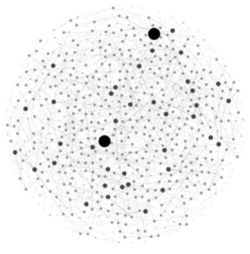
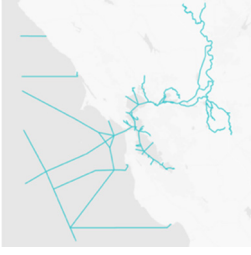





Network Type	Original GIS Data	Geographic Representation	Topographic Representation
Crude Oil Pipeline			
Product Pipeline			
Railway			
Marine Route			
Road (Example: city of Berkeley)			

Table A2. The process of creating connections between all asset types.

Type of Node Asset	Type of Link Asset	Method of Connection	Example
Port	Marine Route	Ports are the endpoints (vertex with degree of one) of marine transportation routes. In the network model, all ports are connect to the nearest marine route vertex.	Port of Stockton, wharf No.9 is connected to the nearest vertex along the marine route.
	Crude Oil Pipeline	Some ports are connected to crude oil pipelines in order to provide crude oil supply directly to refineries. In the network model, a port is connected to crude oil pipeline endpoints if this port is within 200 m radius of that crude pipeline endpoint. The reason is that after a screening of all crude oil pipeline endpoints, all the ports that are connected to crude oil pipeline locates within 200-m radius.	Benicia Industries Wharf No. 95 is connected to the nearby crude oil pipeline endpoint to provide crude oil supply to the Valero Benicia Refinery.
	Product Pipeline	Some ports serve as intermediate transition points to receive and ship petroleum products. Based on a screening of product pipeline endpoints, a majority of the connecting ports locates within 1 km of the product pipeline endpoint. Therefore in the network model, ports are connected to the nearest product pipeline endpoint within 1km radius.	The Tosco Refining barge wharf is connected to product pipelines for the purpose of transporting refined fuel products to other demand locations.
Terminal	Marine Route	Crude oil from out-of-state is delivered to the Bay Area via marine routes to marine terminals for temporary storage purposes. The subset of marine terminals (all marine terminals locates within 1km buffer of marine routes) are selected and then connected to the nearest marine route vertex.	The Andeavor Martinez Refinery receives crude oil by tanker through the San Francisco Bay at the Logistics LP Martinez marine terminal, a third party terminal in Martinez and third-party pipeline systems.
	Crude Oil Pipeline	Crude oil from California is delivered to the coastal refineries by crude oil pipelines via terminals or directly to refineries. Based on existing knowledge on the connection between terminals and crude oil pipelines, we find that all terminals that connect to a crude oil pipeline locate within 500-m radius of the pipeline endpoint. Therefore, in the network model, these terminals are connected to all crude oil pipeline endpoints within 500 m.	Plains Martinez terminal is connected to crude oil pipelines to deliver crude oil to refinery.
	Product Pipeline	Some terminals are directly connected to product pipelines for refined fuel product transmission purposes. Based on existing knowledge on the connections between terminals and product pipelines, we find that all terminals that connect to product pipelines locate within 500-m radius of the pipeline endpoint. Therefore, in the network model, these terminals are connected to all product pipeline endpoints that are within 500 m.	The Kinder Morgan Concord terminal is the biggest fuel terminal in northern California. It is connected to various product pipelines in order to transport refined products from the refineries in Richmond to Brisbane, Sacramento, Chico, Fresno, Stockton, San Jose etc.
	Railway	Railway terminals are transmission locations for crude oil transportation. Based on a screening of the subset of rail terminals, we find that they locate within a 500 m radius of railway endpoints. Therefore, in the network model, rail terminals are connected to all railway endpoints within a 500 m radius.	The BNSF crude rail terminal in Richmond is connected to multiple railway lines to transport crude oil from state oil fields to northern refineries.

Table A2. Cont.

Type of Node Asset	Type of Link Asset	Method of Connection	Example
	Road	Terminals are usually connected to the drivable road network for on/off loading of refined products. In the network model, these terminals are connected to the nearest road network vertex.	The Kinder Morgan Brisbane terminal has racks that could off-load refined fuel products onto tanker trucks for final delivery.
Refinery	Crude Oil Pipeline	Refineries are often directly connected to crude oil pipelines for crude oil supply. In the network model, all five refineries within the study area are connected to crude oil pipeline endpoints based on online and previously conducted interview findings.	The Chevron Richmond refinery is connected to the Richmond Long Wharf via a crude oil pipeline for 100% of its crude input.
	Product Pipeline	Refineries are often connected to product pipelines to transport refined fuel products to other demand locations. In the network model, the refineries are connected to product pipeline endpoints based on online and previously conducted interview findings.	The Chevron Richmond refinery is connected to multiple product pipelines to transport fuel products such as jet fuel to San Francisco airport.
	Railway	Some refineries receive crude oil supply from southern California via railways. Based on interview findings, the crude oil coming into the Bay Area by rail was idle therefore are not considered in network model.	N/A
Gas Station	Road	Gas stations are connected to the road network so that tanker trucks can carry refined fuel products from terminals or refineries to gas stations. Therefore, in the network model, each gas station is connected to the nearest road vertex.	The Shell gas station at 999 San Pablo Ave, Albany is connected to the road network for gasoline and diesel supply.
Airport	Product Pipeline	Airports are big consumers of jet fuel and they are always connected to product pipelines to receive fuel supply. Based on online research and interview findings, we selected San Francisco Airport, Oakland International Airport and San Jose International Airport and connect them to the all product pipeline endpoint within 500 m in the network model.	The San Francisco International Airport is connected to jet fuel product pipeline for its fuel supply.
	Road	Each airport is also connected to the nearest road network vertex in the network model because in real situation, almost all airports are accessible by car.	The San Francisco International Airport is connected to the road network.

References

- Clinton Critical Infrastructure Protection. 1996. Available online: <https://fas.org/irp/offdocs/eo13010.htm> (accessed on 19 May 2021).
- Yusta, J.M.; Correa, G.J.; Lacal-Arántegui, R. Methodologies and Applications for Critical Infrastructure Protection: State-of-the-Art. *Energy Policy* **2011**, *39*, 6100–6119. [[CrossRef](#)]
- Kazemi, Y.; Szmerekovsky, J. Modeling Downstream Petroleum Supply Chain: The Importance of Multi-Mode Transportation to Strategic Planning. *Transp. Res. Part E Logist. Transp. Rev.* **2015**, *83*, 111–125. [[CrossRef](#)]
- Cragg, C.; Burton, A.; Feinberg, E.; Schaik, J. *Energy Fundamentals: Understanding the Oil & Gas Industries*; Energy Intelligence: New York, NY, USA, 2011.
- Herkenhoff, L. The industry profiles collection. In *A Profile of the Oil and Gas Industry: Resources, Market Forces, Geopolitics, and Technology*, 1st ed.; Business Expert Press: New York, NY, USA, 2014; ISBN 978-1-60649-500-1.
- Lindner, C.; Burla, P.; Vallée, D. Graph-Theory-Based Modeling of Cascading Infrastructure Failures. *J. Extr. Even.* **2018**, *4*, 1750012. [[CrossRef](#)]
- Nieuwenhuijs, A.; Luijff, E.; Klaver, M. Modeling Dependencies in Critical Infrastructures. In *Critical Infrastructure Protection II*; Papa, M., Sheno, S., Eds.; Springer: Boston, MA, USA, 2008; pp. 205–213.
- Amin Massoud Toward Secure and Resilient Interdependent Infrastructures. *J. Infrastruct. Syst.* **2002**, *8*, 67–75. [[CrossRef](#)]

9. IPCC IPCC—SREX. Available online: <http://www.ipcc.ch/report/srex/> (accessed on 23 February 2018).
10. IPCC IPCC. Fifth Assessment Report. Available online: <https://www.ipcc.ch/report/ar5/> (accessed on 19 February 2018).
11. Keener, V. *Regional Climate Scenarios and Trends for the U.S. National Climate Assessment. Part 8: Climate of the Pacific Islands*; CreateSpace Independent Publishing Platform: Scotts Valley, CA, USA, 2015; ISBN 978-1-5141-9690-8.
12. National Academies of Sciences, Engineering, and Medicine. *Attribution of Extreme Weather Events in the Context of Climate Change*; National Academies Press: Washington, DC, USA, 2016; ISBN 978-0-309-38094-2.
13. Peterson, T.C.; Stott, P.A.; Herring, S. Explaining Extreme Events of 2011 from a Climate Perspective. *Bull. Am. Meteorol. Soc.* **2012**, *93*, 1041–1067. [[CrossRef](#)]
14. Vose, S.R.; Applequist, S.; Bourassa, M.; Pryor, S.; Barthelmie, R.; Blanton, B.; Bromirski, P.; Brooks, H.; Degaetano, A.; Dole, R.; et al. Monitoring and Understanding Changes in Extremes: Extratropical Storms, Winds, and Waves. *Bull. Am. Meteorol. Soc.* **2014**, *93*, 377–386. [[CrossRef](#)]
15. UN, Climate Change Cancun Climate Change Conference—November 2010. Available online: http://unfccc.int/meetings/cancun_nov_2010/meeting/6266.php (accessed on 19 February 2018).
16. Mazo, J. Climate Change Impacts in the United States: The Third National Climate Assessment. *Survival* **2014**, *56*, 175–183. [[CrossRef](#)]
17. National Climate Assessment National Climate Assessment. Available online: <https://nca2014.globalchange.gov/node/1961> (accessed on 19 February 2018).
18. He, Y.; Thies, S.; Avner, P.; Rentschler, J. Flood Impacts on Urban Transit and Accessibility—A Case Study of Kinshasa. *Transp. Res. Part D Transp. Environ.* **2021**, *96*, 102889. [[CrossRef](#)]
19. Smith, A.B.; Katz, R.W. US Billion-Dollar Weather and Climate Disasters: Data Sources, Trends, Accuracy and Biases. *Nat Hazards* **2013**, *67*, 387–410. [[CrossRef](#)]
20. Smith, A.B.; Matthews, J.L. Quantifying Uncertainty and Variable Sensitivity within the US Billion-Dollar Weather and Climate Disaster Cost Estimates. *Nat. Hazards* **2015**, *77*, 1829–1851. [[CrossRef](#)]
21. Lott, J.N.; Tracking and Evaluating U.S. Billion Dollar Weather Disasters. Available online: https://ams.confex.com/ams/Annual2006/techprogram/paper_100686.htm (accessed on 19 February 2018).
22. Radke, J.D.; Biging, G.S.; Roberts, K.; Schmidt-Poolman, M.; Foster, H.; Roe, E.; Ju, Y.; Lindbergh, S.; Beach, T.; Maier, L.; et al. Assessing Extreme Weather-Related Vulnerability and Identifying Resilience Options for California’s Interdependent Transportation Fuel Sector. In *California’s Fourth Climate Change Assessment*; California Energy Commission; University of California: Berkeley, CA, USA, 2018; Publication number: CCCA4-CEC-2018-012. Available online: https://www.energy.ca.gov/sites/default/files/2019-11/Energy_CCCA4-CEC-2018-012_ADA.pdf (accessed on 10 August 2021).
23. Shirzaei, M.; Bürgmann, R. Global Climate Change and Local Land Subsidence Exacerbate Inundation Risk to the San Francisco Bay Area. *Sci. Adv.* **2018**, *4*, eaap9234. [[CrossRef](#)]
24. Griggs, G.; Cayan, D.; Tebaldi, C.; Fricker, H.; Árvai, J.; DeConto, R.; Kopp, R.; Whiteman, L.; Moser, S.; Fox, J. Rising Seas in California: An Update on Sea-Level Rise Science. 2017. Available online: <https://cnap.ucsd.edu/2017/05/30/sea-level-rise-resources-for-california/> (accessed on 22 June 2021).
25. Mallick, R.; Radzicki, M.; Daniel, J.; Jacobs, J. Use of System Dynamics to Understand Long-Term Impact of Climate Change on Pavement Performance and Maintenance Cost. *Transp. Res. Rec. J. Transp. Res. Board* **2014**, *2455*, 1–9. [[CrossRef](#)]
26. Schweikert, A.; Espinet, X.; Goldstein, S.; Chinowsky, P. Resilience versus Risk. *Transp. Res. Rec. J. Transp. Res. Board* **2015**, *2532*, 13–20. [[CrossRef](#)]
27. Barnard, P.L.; Erikson, L.H.; Foxgrover, A.C.; Hart, J.A.F.; Limber, P.; O’Neill, A.C.; van Ormondt, M.; Vitousek, S.; Wood, N.; Hayden, M.K.; et al. Dynamic Flood Modeling Essential to Assess the Coastal Impacts of Climate Change. *Sci. Rep.* **2019**, *9*, 4309. [[CrossRef](#)] [[PubMed](#)]
28. Cayan, D.R.; Bromirski, P.D.; Hayhoe, K.; Tyree, M.; Dettinger, M.D.; Flick, R.E. Climate Change Projections of Sea Level Extremes along the California Coast. *Clim. Chang.* **2008**, *87*, 57–73. [[CrossRef](#)]
29. EIA Form EIA-923 Detailed Data with Previous Form Data (EIA-906/920). Available online: <https://www.eia.gov/electricity/data/eia923/> (accessed on 22 June 2021).
30. NOAA Regional Climate Trends and Scenarios for the U.S. National Climate Assessment: Part 7. Climate of Alaska | CAKE: Climate Adaptation Knowledge Exchange. Available online: <http://www.cakex.org/virtual-library/regional-climate-trends-and-scenarios-us-national-climate-assessment-part-7-climate> (accessed on 27 February 2018).
31. Wilbanks, T.J.; Fernandez, S. Framing Climate Change Implications for Infrastructures and Urban Systems. In *Climate Change and Infrastructure, Urban Systems, and Vulnerabilities*; NCA Regional Input Reports; Island Press: Washington, DC, USA, 2014; pp. 17–40. ISBN 978-1-59726-469-3.
32. *Building a Resilient Energy Gulf Coast: Executive Report*; Entergy Corporation: New Orleans, LA, USA, 2010.
33. Rosenzweig, C.; Solecki, W. New York City Panel on Climate Change (NPCC) Climate Risk Information 2013—Observations, Climate Change Projections, and Maps | Adaptation Clearinghouse. Available online: <http://www.adaptationclearinghouse.org/resources/new-york-city-panel-on-climate-change-npcc-climate-risk-information-2013-observations-climate-change-projections-and-maps.html> (accessed on 23 February 2018).
34. Stelling, G.S. Quadtree Flood Simulations with Sub-Grid Digital Elevation Models. *Proc. Inst. Civ. Eng. Water Manag.* **2012**, *165*, 567–580. [[CrossRef](#)]

35. Schuurman, W.; Leeuwen, E. *3Di: A New Dutch Hydrological Model*; 3Di Water Management: Utrecht, The Netherlands, 2017; Available online: https://3diwatermanagement.com/wp-content/uploads/2019/02/3Di_A-new-dutch-integrated-model-19-oct-2017.pdf (accessed on 9 August 2021).
36. Ju, Y.; Lindbergh, S.; He, Y.; Radke, J.D. Climate-Related Uncertainties in Urban Exposure to Sea Level Rise and Storm Surge Flooding: A Multi-Temporal and Multi-Scenario Analysis. *Cities* **2019**, *92*, 230–246. [[CrossRef](#)]
37. Cayan, D.R.; Kalansky, J.; Iacobellis, S.; Pierce, D. *Creating Probabilistic Sea Levee Rise Projections to Support the 4th California Climate Assessment*; California Energy Commission: Sacramento, CA, USA, 2016.
38. Fourth Assessment Report—Climate Change 2007—The Physical Science Basis. Available online: <https://www.ipcc.ch/report/ar4/wg1/> (accessed on 23 February 2018).
39. Kopp, R.E.; Horton, R.M.; Little, C.M.; Mitrovica, J.X.; Oppenheimer, M.; Rasmussen, D.J.; Strauss, B.H.; Tebaldi, C. Probabilistic 21st and 22nd Century Sea-Level Projections at a Global Network of Tide-Gauge Sites. *Earth's Future* **2014**, *2*, 2014EF000239. [[CrossRef](#)]
40. DeConto, R.M.; Pollard, D. Contribution of Antarctica to Past and Future Sea-Level Rise. *Nature* **2016**, *531*, 591–597. [[CrossRef](#)]
41. Cosnet Multiplex Networks 2020.
42. Nicosia, V.; Bianconi, G.; Latora, V.; Barthelemy, M. Growing Multiplex Networks. *Phys. Rev. Lett.* **2013**, *111*, 058701. [[CrossRef](#)] [[PubMed](#)]
43. Bianconi, G. Statistical Mechanics of Multiplex Networks: Entropy and Overlap. *Phys. Rev. E Stat. Nonlinear Soft Matter Phys.* **2013**, *87*, 062806. [[CrossRef](#)] [[PubMed](#)]
44. Hagberg, A.A.; Schult, D.A.; Swart, P.J. Exploring network structure, dynamics, and function using NetworkX. In Proceedings of the 7th Python in Science Conference (SciPy2008), Pasadena, CA, USA, 19–24 August 2008; pp. 11–15.
45. Pregnotato, M.; Ford, A.; Wilkinson, S.M.; Dawson, R.J. The Impact of Flooding on Road Transport: A Depth-Disruption Function. *Transp. Res. Part D Transp. Environ.* **2017**, *55*, 67–81. [[CrossRef](#)]
46. Latora, V.; Marchiori, M. Efficient Behavior of Small-World Networks. *Phys. Rev. Lett.* **2001**, *87*, 198701. [[CrossRef](#)]
47. Osei-Asamoah, A.; Lownes, N. Complex Network Method of Evaluating Resilience in Surface Transportation Networks. *Transp. Res. Rec. J. Transp. Res. Board* **2014**, *2467*, 120–128. [[CrossRef](#)]
48. DHS National Infrastructure Protection Plan (NIPP) 2013: Partnering for Critical Infrastructure Security and Resilience. 2013. Available online: <https://www.cisa.gov/publication/nipp-2013-partnering-critical-infrastructure-security-and-resilience> (accessed on 22 June 2021).
49. DHS National Infrastructure Protection Plan (NIPP) 2015: Energy Sector-Specific Plan 2015. Available online: <https://www.cisa.gov/publication/nipp-ssp-energy-2015> (accessed on 22 June 2021).
50. CalOES. Emergency Transportation Fuels Set-A-Side Program. Discussion Based Table Top Exercise. Participant Handbook. 2016. Available online: <https://www.naseo.org/Data/Sites/1/fuels-set-a-side-participant-handbook.pdf> (accessed on 22 June 2021).
51. Hilyard, J. *The Oil & Gas Industry: A Nontechnical Guide*; PennWell Corporation: Tulsa, OK, USA, 2012; Available online: <http://site.ebrary.com/lib/berkeley/reader.action?docID=10605558&ppg=1> (accessed on 2 January 2018).
52. California Energy Commission California's Oil Refineries. Available online: http://www.energy.ca.gov/almanac/petroleum_data/refineries.html (accessed on 23 March 2018).
53. Rodrigue, J.-P.; Comtois, C.; Slack, B. *The Geography of Transport Systems*, 4th ed.; Routledge: London, UK, 2017.
54. Boven, K. Chevron Richmond Long Wharf—A MOTEMS Journey 2014. Available online: http://www.slc.ca.gov/About/Prevention_First/2014/MOTEMS-Chevron.pdf (accessed on 30 April 2018).
55. California Energy Commission California Retail Fuel Outlet Annual Reporting (CEC-A15) Results. Available online: http://www.energy.ca.gov/almanac/transportation_data/gasoline/piira_retail_survey.html (accessed on 2 January 2018).
56. California Department of Transportation. *California Military Use Airports*; Caltrans GIS Data: Sacramento, CA, USA, 2012. Available online: http://www.dot.ca.gov/hq/tsip/gis/datalibrary/Metadata/Airp_military.html (accessed on 2 January 2018).
57. Pipeline and Hazardous Materials Safety Administration National Pipeline Mapping System. Available online: <https://www.npms.phmsa.dot.gov/GeneralPublic.aspx> (accessed on 2 January 2018).